Acta Biomaterialia 58 (2017) 337–348

Contents lists available at ScienceDirect

Acta Biomaterialia

journal homepage: www.elsevier.com/locate/actabiomat

Full length article

Transcriptome profiling of 3D co-cultured cardiomyocytes and endothelial cells under oxidative stress using a photocrosslinkable hydrogel system

Xiaoshan Yue [a], Aylin Acun [b], Pinar Zorlutuna [a,b,*]

[a] University of Notre Dame, Department of Aerospace and Mechanical Engineering, Bioengineering Graduate Program, United States
[b] University of Notre Dame, Bioengineering Graduate Program, United States

ARTICLE INFO

Article history:
Received 22 February 2017
Received in revised form 20 June 2017
Accepted 21 June 2017
Available online 23 June 2017

Keywords:
Photocrosslinkable hydrogel
3D co-culture
Cardiomyocytes
Oxidative stress
Transcriptome

ABSTRACT

Myocardial infarction (MI) is one of the most common among cardiovascular diseases. Endothelial cells (ECs) are considered to have protective effects on cardiomyocytes (CMs) under stress conditions such as MI; however, the paracrine CM-EC crosstalk and the resulting endogenous cellular responses that could contribute to this protective effect are not thoroughly investigated. Here we created biomimetic synthetic tissues containing CMs and human induced pluripotent stem cell (hiPSC)-derived ECs (iECs), which showed improved cell survival compared to single cultures under conditions mimicking the aftermath of MI, and performed high-throughput RNA-sequencing to identify target pathways that could govern CM-iEC crosstalk and the resulting improvement in cell viability. Our results showed that single cultured CMs had different gene expression profiles compared to CMs co-cultured with iECs. More importantly, this gene expression profile was preserved in response to oxidative stress in co-cultured CMs while single cultured CMs showed a significantly different gene expression pattern under stress, suggesting a stabilizing effect of iECs on CMs under oxidative stress conditions. Furthermore, we have validated the *in vivo* relevance of our engineered model tissues by comparing the changes in the expression levels of several key genes of the encapsulated CMs and iECs with *in vivo* rat MI model data and clinical data, respectively. We conclude that iECs have protective effects on CMs under oxidative stress through stabilizing mitochondrial complexes, suppressing oxidative phosphorylation pathway and activating pathways such as the drug metabolism-cytochrome P450 pathway, *Rap1* signaling pathway, and adrenergic signaling in cardiomyocytes pathway.

Statement of Significance

Heart diseases are the leading cause of death worldwide. Oxidative stress is a common unwanted outcome that especially occurs due to the reperfusion following heart attack or heart surgery. Standard methods of *in vivo* analysis do not allow dissecting various intermingled parameters, while regular 2D cell culture approaches often fail to provide a biomimetic environment for the physiologically relevant cellular phenotypes. In this research, a systematic genome-wide transcriptome profiling was performed on myocardial cells in a biomimetic 3D hydrogel-based synthetic model tissue, for identifying possible target genes and pathways as protecting regulators against oxidative stress. Identification of such pathways would be very valuable for new strategies during heart disease treatment by reducing the cellular damage due to reperfusion injury.

1. Introduction

Myocardial infarction (MI) is one of the most prevalent cardiovascular diseases (CVDs), affecting millions of people and costing billions of dollars in healthcare expenditures every year [1]. Heart tissue has endogenous processes in the early stages and in the

* Corresponding author at: 143 Multidisciplinary Research Building, University of Notre Dame, Notre Dame, IN 46556, United States.
E-mail address: Pinar.Zorlutuna.1@nd.edu (P. Zorlutuna).

http://dx.doi.org/10.1016/j.actbio.2017.06.031
1742-7061/

aftermath of the MI that could confer cardioprotection. The cell-cell interactions of cardiomyocytes with cardiac fibroblasts [2,3] and endothelial cells [4] are shown to have a protective effect against ischemia-reperfusion injury. Traditionally, ECs had been regarded as a barrier for transport. However, the discovery of involvement of microvascular ECs in the regulation of heart tissue led to their reclassification as myocardial regulators [5]. Some of the microvascular EC-driven modulators have been identified as nitric oxide (NO), endothelin 1 (ET-1), angiopoietin-II, and prostaglandin I2 [6]. The effects of these factors are mostly paracrine, sometimes autocrine, and are particularly effective around the myocardial capillaries where ECs directly interact with adjacent CMs. It is also known that this interaction is bidirectional and CMs release factors such as vascular endothelial growth factor (VEGF) and angiopoietin-I, which also modulate EC behavior [7]. Interactions between ECs and CMs in heart tissue are not restricted to the control of myocardial contractility but also involved in development [8,9], growth [10], function [11], and changes in its metabolism under pathophysiological conditions [12–14]. The effects of the EC-generated factors are more pronounced during abnormal physiological conditions, such as hypoxia, oxygen tension, abnormal blood flow, and inflammation. Beginning with the early stages of MI, all of these major cardiovascular risk factors may cause ECs to start interacting with the CMs to help the heart tissue adapt to the changing microenvironment.

One of the traditional methods to study paracrine effects of one cell type on another is to transfer conditioned media between the culture wells [15]. However, this method is time consuming and sometimes misleading due to the lack of any crosstalk between different cell types. Another way is to use the transwell co-culture system in which different types of cells are separated by a transwell insert. However, the transwell systems are mostly applied in 2D cultures, which have limitations for representing the *in vivo* microenvironment. In addition, the relatively short half-life of many of the paracrine factors important in EC-CM communication, such as NO, ET-1, or neuregulin-1, made it challenging to estimate the effects of these paracrine factors with conditioned media or using the transwell system [16–18].

Hydrogels are one of the most common material types that could be used to mimic the *in vivo* microenvironment due to their resemblance to fully hydrated native ECM. Polyethylene glycol (PEG), a synthetic polymer inside which cells cannot proliferate or migrate, is widely used for tissue engineering applications. This synthetic polymer can be modified to improve cell-ECM interactions through incorporating Arginine-Glycine-Aspartic acid (RGD) sequences, and can be photo-responsive through incorporating methacrylate groups. In this study, a 5 to 1 mixture of 4-arm PEG acrylate (4-arm PEG-ACRL, 20 kDa) to RGD modified 4-arm PEG-ACRL (4-arm PEG-ACRL-RGD), respectively, was used to fabricate the hydrogels for 3D co-culture of human induced pluripotent stem cell (hiPSC)-derived ECs (iECs) with CMs, and used as a model system to test the protective effects of paracrine communication between the CMs and iECs in response to oxidative stress. The hiPSC-derived cardiomyocytes (iCMs) are a promising cell source for generating engineered myocardial tissue models [19–22]. Many researches, including our lab [22], investigate how to generate functionally mature iCMs that can be used in model tissue applications. However, at the current stage, the maturity and functionality of the iCMs are still questionable [23]. On the contrary, as a well characterized source for cardiomyocytes, neonatal rat cardiomyocytes are widely used for *in vitro* studies for cardiac pathophysiology, and in co-culture with human ECs in literature for studying various aspects of CM-EC crosstalk [5,14,24]. In this study, we encapsulated neonatal rat CMs and human iECs in photocrosslinkable 4-arm PEG-ACRL/4-arm PEG-ACRL-RGD 3D hydrogels, and performed transcriptome analysis of the encapsulated cells, to assess the responses of CMs to post-MI level oxidative stress with or without the presence of iECs. We eliminated the physical cell-cell contact by using the 4-arm PEG-ACRL/4-arm PEG-ACRL-RGD-based hydrogel system, thus our observations reflect the effect of intercellular crosstalk through paracrine factors only. Although very similar at protein level due to codon degeneracy, rats and humans have distinct DNA sequences that could be used to differentiate them easily at mRNA level [25]. Therefore, by co-culturing rat CMs and human iECs we were able to distinguish between the gene expression changes happening in CMs versus iECs specifically. We found that the iECs conferred a stabilizing effect on CM gene expression upon exposure to post-MI levels of oxidative stress. Furthermore, we have validated the *in vivo* relevance of our engineered model tissues by comparing the changes in the expression levels of several key genes of the encapsulated CMs and iECs with *in vivo* rat MI model data and clinical data, respectively. The results of this study will be important for identifying targets for future mechanistic studies of CM-iEC crosstalk, and could potentially lead to new therapeutic targets for MI prevention and treatment.

2. Materials and methods

Details are available in the Online Data Supplement.

2.1. 3D cell culture and oxidative stress treatment

Neonatal rat CMs were isolated from 2-day-old Sprague-Dawley rats (Charles River Laboratories) using a previously established protocol [26]. All experiments were conducted in accordance to the Institutional Animal Care and Use Committee of the University of Notre Dame. The hiPSCs were cultured in mTeSR1 media (Stemcell Technologies) using Geltrex (Life Technologies) coated tissue culture dishes with daily media changes. The iECs were differentiated from hiPSCs following a protocol that yields 99% purity as described previously [27]. Cell-laden hydrogels were fabricated by encapsulating CMs and iECs in a mixture containing 85% of 4-arm PEG-ACRL (JenKem Technology) and 15% of RGD (Bachem) conjugated 4-arm PEG-ACRL (4-arm PEG-ACRL-RGD) ($n = 3$). CMs were encapsulated either alone at a density of $9x10^5$ cells per construct, or mixed with $2x10^5$ iECs per construct during the encapsulation process, for single culture and co-culture experiments, respectively. Photo-crosslinking was initiated by exposure to 6.9 mW/cm^2 UV irradiation (320-500 nm) for 20 s. 0.1% w/v 2-hydroxy-1-(4-(hydroxyethoxy) phenyl)-2-methyl-1-propanone (Irgacure 2959, BASF Corporation) was added as photoinitiator. The high UV dose rate and short exposure time assures minimal oxidative stress and cell damage caused by UV exposure [28,29]. Oxidative stress was applied to the treatment group by incubating in standard culture media containing 0.2 mM H_2O_2 for 16 h, followed by 2 h incubation in normoxic standard culture media. The control group was incubated in normoxic media for 18 h in total, with a media change at 16 h.

2.2. RNA-sequencing

Libraries were prepared from total RNA isolated from the single culture and co-culture cell-laden hydrogels using the Illumina TruSeq stranded mRNA library preparation kit. Quality check and quantitation was performed using a combination of Qubit dsDNA assay, Caliper LabChipGX size determination and Kapa Biosystems Illumina Library qPCR assay. Illumina HiSeq 2500 Rapid Run flow cell (v2) was used for sequencing with HiSeq Rapid SBS reagents (v2) in a 2 × 100 bp paired end format. Illumina Real Time Analysis (RTA) (v1.18.64) was used for base calling.

2.3. Data analysis

RNA-sequencing data were screened and analyzed with in house generated R code. Kyoto Encyclopedia of Genes and Genomes (KEGG) pathway analysis was done with R package Cluster Profiler [30]. Network analysis of significantly changed genes was performed with Search Tool for the Retrieval of Interacting Genes/Proteins (STRING) [31].

2.4. Statistical analysis

Data was analyzed for statistical significance using one-way ANOVA test or Student's *t*-test ($^{*}p < 0.01$, $^{**}p < 0.001$, $^{***}p < 0.0001$). Error bars represent mean ± standard deviation (SD).

3. Results

3.1. Fabrication and characterization of 4-arm PEG-ACRL/4-arm PEG-ACRL-RGD cell-laden hydrogels for 3D co-culture

Cell-laden hydrogels were fabricated as shown in Fig. 1A. The stiffness of the 4-arm PEG-ACRL/4-arm PEG-ACRL-RGD hydrogels without any cell encapsulation was measured over a 14-day period using a nanoindentor, to ensure a stable biomimetic physical microenvironment for the encapsulated cells. The results showed a steady stiffness of 8 kPa up to 14 days for the hydrogel under cell culture conditions (Fig. 1B). We also examined the stiffness of the cell-laden hydrogels, which had a slightly higher stiffness around 10 kPa (Supplementary Fig. 1), that is within the stiffness range of 10–15 kPa of normal cardiac muscle tissue [32]. In addition, the stiffness of hydrogel-based model tissues was not affected by the encapsulated cell density. Even with a 100 times increase of encapsulation density, the stiffness of model tissues remained constant at around 10 kPa (Supplementary Fig. 1). To test 4-arm PEG-ACRL/4-arm PEG-ACRL-RGD hydrogel's ability in restraining cell proliferation and migration for studying paracrine interactions reliably, we tracked the locations and numbers of encapsulated neonatal rat cardiac fibroblasts, the cell type that has the highest proliferative and migratory capacity in the native heart tissue. Cardiac fibroblasts were stained with live/dead stain and imaged in 3D using a fluorescence microscope with z-stacking capabilities on day 1 and day 7 after the encapsulation. The cell numbers and the distance between the cells were measured using the z-stack slices and ImageJ (Fig. 1C–F). Cell numbers showed no statistically significant difference during the 7 days of culture in 4-arm PEG-ACRL/4-arm PEG-ACRL-RGD, indicating the lack of cell proliferation as expected (Fig. 1D). In addition, the distribution of intercellular distance showed the similar trend on day 1 and day 7, with the highest distribution of nearest neighbor distance measured being 10–30 μm (Fig. 1E–F). These results showed that the 4-arm PEG-ACRL/4-arm PEG-ACRL-RGD hydrogels can be used as a culture system with biomimetic properties that resembles the native heart tissue, and can maintain the cell number and distribution without permitting cell growth or cell migration, thus can be used as a suitable system for evaluating paracrine effects *in vitro*.

3.2. CMs co-cultured with iECs in 3D biomimetic hydrogels showed improved viability and fewer changes in their gene expression profile in response to oxidative stress

We applied post-MI level oxidative stress to the cell-laden hydrogels through H_2O_2 (0.2 mM) exposure as illustrated in Fig. 1A. Cell viability of the constructs with or without oxidative stress was assessed with live/dead staining (Fig. 1G), and the live cell percentages were calculated by dividing the live cell numbers by the total cell numbers. Both CMs and iECs were sensitive to H_2O_2 exposure in single culture, with the cell viability decreased from 71.4% to 41.2% for CMs (decreased by 30.2%), and from 77.7% to 59.8% for iECs (decreased by 17.9%). In comparison, in the co-culture system, the cells showed less sensitivity in response to H_2O_2 exposure compared to the ones in single culture, with the viability decrease from 81.4% to 66.9% (decreased by 14.9%) (Fig. 1H). In our biomimetic 3D hydrogel-based synthetic model tissues, the iECs cannot proliferate and the iEC/CM ratio stays constant, so that there is no concern of iECs overgrowing CMs in the 3D tissue constructs. We used an iEC to CM ratio of 1 to 4 for constructing the co-culture model tissue, to assure that the increase in cell survival in the co-culture is not merely due to the surviving iECs, but due to improved CM viability. In addition, the 4-arm PEG-ACRL/4-arm PEG-ACRL-RGD 3D model tissues kept the iEC to CM ratio constant throughout the experiment, ensuring that the iECs, which are more resilient to stress, do not take over the culture. Taken together, these results indicate a protective effect of the co-culture condition on the CMs as we have investigated in detail in our recent publication [33].

In order to evaluate the crosstalk between CMs and iECs in response to oxidative stress, the transcriptome of CMs in single culture or in the co-culture with iECs with or without H_2O_2 treatment were profiled and screened for significantly changed genes. The conditions compared were as follows: 1) 3D single cultured CMs without oxidative stress (CM-N); 2) 3D single cultured CMs with oxidative stress (CM-S); 3) 3D co-cultured CMs and iECs without oxidative stress (CMEC-N); and 4) 3D co-cultured CMs and iECs with oxidative stress (CMEC-S). The gene expression levels of each condition were normalized to the CM-N condition and genes with more than a 2-fold change in expression levels and a *p*-value less than 0.05 in any of the conditions were considered significantly changed to ensure high confidence (Fig. 2A, Supplemental Table 1). In this study, the iECs were of human origin while CMs were of rat origin. Thus, it was possible to distinguish the gene expression changes in iECs from those in CMs within the co-culture group. It should be noted that many of the proteins that could be involved in CM-iEC crosstalk are homologous in rats and humans, although they have distinct mRNA sequences [25]. Therefore, we were able to compare the gene expression profiles of iECs in the CM-iEC co-culture system with or without oxidative stress treatments.

The gene expression profile of CMs under CMEC-N and CMEC-S conditions showed many similarities, while the gene profiles of CMs under CM-S and CMEC-S conditions were completely different, indicating that co-culturing was a more significant factor than oxidative stress for affecting CMs' gene expression patterns. Furthermore, our result suggested that CMs were protected against oxidative stress by co-culturing with iECs, and their gene expression profile was stabilized in co-culture in response to oxidative stress. This conclusion was supported by the fact that the difference between gene expression profiles of CMEC-N and CMEC-S was much smaller than the difference between CM-N and CM-S, with 138 significantly changed genes versus 467, respectively. The box plots showed that most of the genes in CM-S group had a -2 to 3-fold-change in $\log_2$ scale, while most of the co-culture groups had a -4 to 2-fold-change in $\log_2$ scale (Fig. 2B). In the co-culture groups, some genes fell far beyond the top whisker, indicating these genes were remarkably affected by the co-culture condition. The most remarkably upregulated gene in the co-culture groups was *LOC100911132*, which had glutamine-tRNA ligase and ATP binding activity. The second most remarkably upregulated gene in the co-culture groups was guanine nucleotide binding protein (G protein) beta polypeptide 2-like 1 (*Gnb2l1*), which was related to G-protein-coupled receptors (GPCR) and extracellular signal-regulated kinase (ERK) signaling, and was related to poly

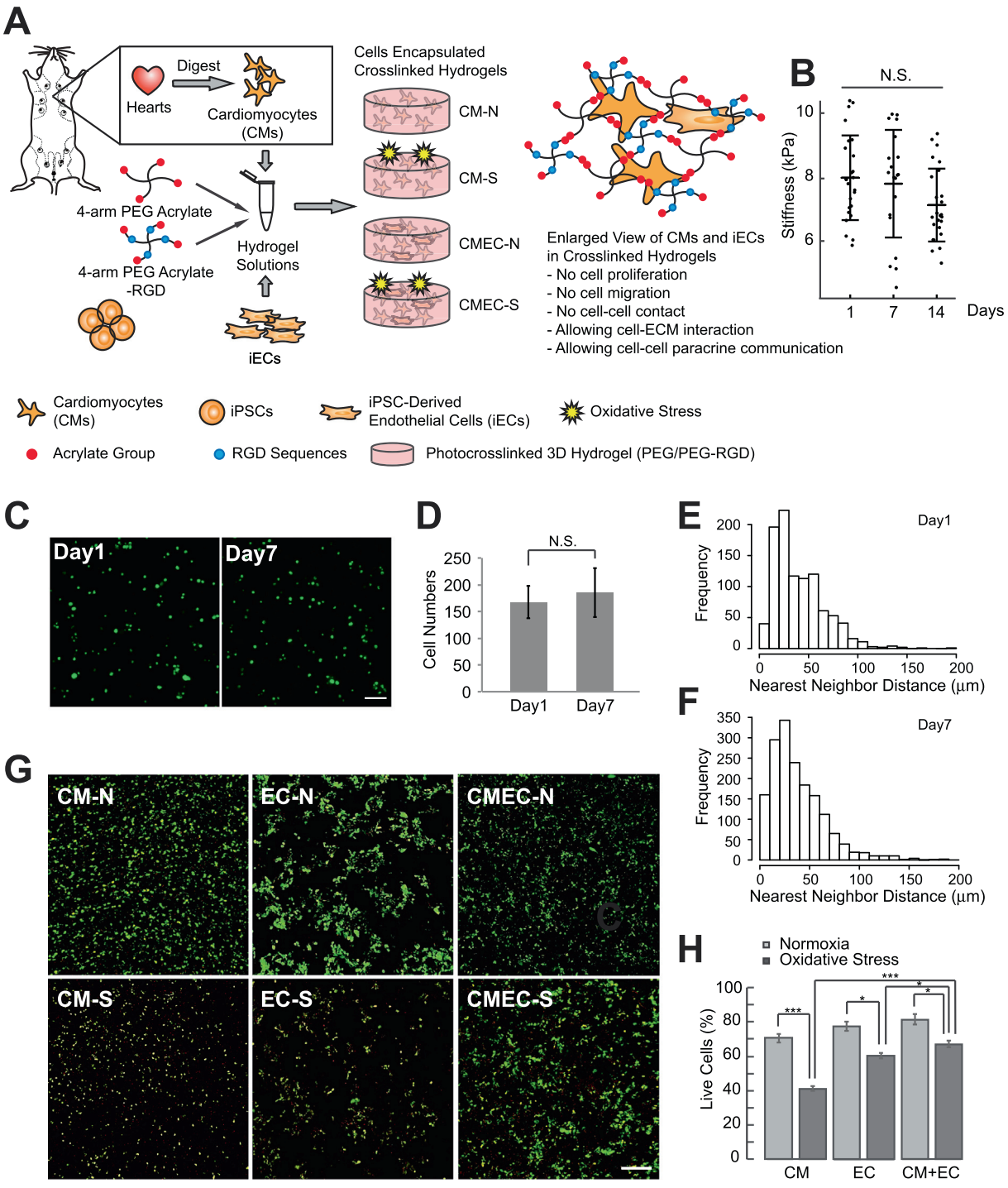

Fig. 1. 3D culture model using 4-arm PEG-ACRL/4-arm PEG-ACRL-RGD hydrogels. A) Illustration of the co-cultured cells in 4-arm PEG-ACRL/4-arm PEG-ACRL-RGD hydrogels. CM-N: 3D single cultured CMs without oxidative stress; CM-S: 3D single cultured CMs with oxidative stress; CMEC-N: 3D co-cultured CMs and iECs without oxidative stress; CMEC-S: 3D co-cultured CMs and iECs with oxidative stress. B) Stiffness of 4-arm PEG-ACRL/4-arm PEG-ACRL-RGD hydrogels over 14 days of incubation. C) Fluorescence staining of live cardiac fibroblasts on day 1 and day 7 after encapsulated in 4-arm PEG-ACRL/4-arm PEG-ACRL-RGD hydrogels. D) Live cardiac fibroblast numbers on day 1 and day 7 after encapsulated in 4-arm PEG-ACRL/4-arm PEG-ACRL-RGD hydrogels. E), F) Distribution of nearest neighbor distance between living cardiac fibroblasts on day 1 (E) and day 7 (F) after encapsulated in 4-arm PEG-ACRL/4-arm PEG-ACRL-RGD hydrogels. G) Live/dead staining of rat CMs, human iECs, and their co-cultures encapsulated in 4-arm PEG-ACRL/4-arm PEG-ACRL-RGD hydrogels with or without oxidative stress treatment. H) Live cell percentage of rat CMs, human iECs, and the co-cultured cells encapsulated in 4-arm PEG-ACRL/4-arm PEG-ACRL-RGD hydrogels with or without oxidative stress treatment. $^{*}p < 0.01$; $^{***}p < 0.0001$; N.S.: no statistically significant differences. Scale bar = 100 μm.

(A) RNA binding and receptor binding. These two most remarkably upregulated genes showed similar expression levels in CMEC-N and CMEC-S groups, indicating that the changes in the expression levels of these genes were caused primarily by the co-culture condition with iECs and not much affected by the applied oxidative stress. In addition to these two most remarkably affected genes, 23 genes fell beyond the top whisker in the CMEC-N group, and among them, 21 had similar expression levels in CMEC-N and CMEC-S conditions, further suggesting that gene expression changes mediated by the CM-iEC crosstalk were maintained upon

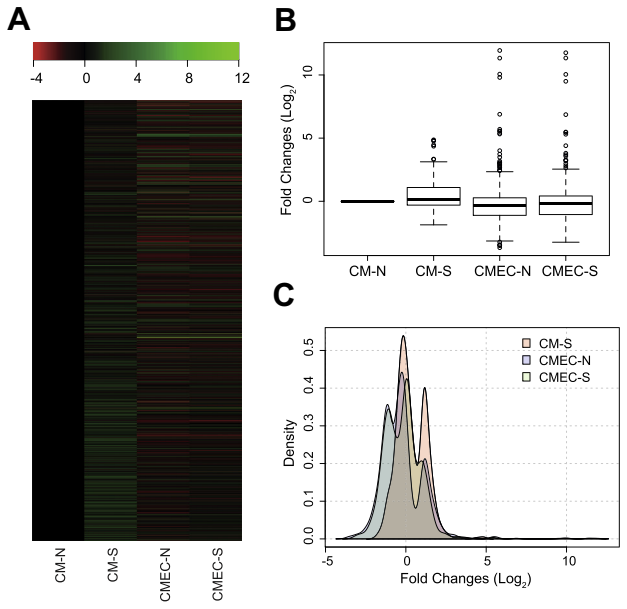

Fig. 2. Gene expression distribution. A) Heatmap of gene expression changes in 1) 3D single cultured CMs without oxidative stress (CM-N); 2) 3D single cultured CMs with oxidative stress (CM-S); 3) 3D co-cultured CMs and iECs without oxidative stress (CMEC-N); and 4) 3D co-culture CMs and iECs with oxidative stress (CMEC-S). All gene expressions were normalized to CM-N. B) Box plot showing the gene expression distributions. The middle line indicates the median of the gene expression. Circles indicate the genes out of the range from first quartile (Q1) minus 1.5 times interquartile range (IQR) to third quartile (Q3) plus 1.5 times IQR. C) Fitted distribution curves of genes that have changed significantly under CM-S, CMEC-N, and CMEC-S. All genes were screened with p-value < 0.05 and more than 2-fold expression changes.

oxidative stress challenge. These 21 genes (Supplementary Table 1, with $\log_2$ fold-change > 2.5 for CMEC-N) could have important roles in cardioprotection, and should be investigated further. The distributions of expression levels of significantly changed genes in CM-S, CMEC-N, and CMEC-S were further assessed using histogram analysis (Fig. 2C). The gene expression distributions of in CMEC-N and CMEC-S conditions showed a large overlap, and both of them had more balanced distribution compared to CM-S, which showed a large peak corresponding to upregulation with the $\log_2$ fold-change centered at around 2 (Fig. 2C, red curve). In contrast, the CMEC-N and CMEC-S distribution showed two peaks at both downregulation and upregulation regions.

In summary, these results showed that, as expected, co-culturing with iECs altered the gene expression profile of the CMs. In addition, the oxidative stress challenge caused significant changes in the gene expression profile of the CMs that were cultured alone, most of which were upregulations. Interestingly, the number of genes that were upregulated in response to oxidative stress was significantly lower in the presence of iECs, as indicated by the expression profile of CMEC-S, suggesting a stabilization effect on CMs by CM-iEC crosstalk, which is in accordance with the higher cell viability we observed in the co-culture condition in response to oxidative stress as shown in Fig. 1G and H.

3.3. CM genes with expression profile changes were classified into three clusters

In order to further examine the changes in the gene expression patterns of the CMs, the significantly changed genes were classified with k-means method, which identified 3 clusters (Fig. 3A). The 3 clusters were clearly separated from each other with almost no mixing at the boundary. As shown in Fig. 3B, cluster 1 included genes that were mostly downregulated in CMEC-N and CMEC-S, and the changes in CM-S were less remarkable and had no specific trend towards up- or downregulation (Supplemental Table 2). Cluster 2 included genes that were upregulated in CMEC-N and CMEC-S, and the expression changes in CM-S in this cluster were less remarkable and were without any specific trend (Supplemental Table 3). Cluster 3 included genes that were upregulated in CM-S. In this cluster, the genes in CMEC-N and CMEC-S were either downregulated or kept at a similar expression level as CM-N, and did not show as much upregulation as in CM-S (Supplemental Table 4). Heatmaps of the three clusters (Fig. 3C) showed similar gene expression trends as those shown in Fig. 3B. From these results, it can be concluded that the CMEC-N and CMEC-S shared very similar gene expression levels and had similar trends for gene up- or downregulation. Clusters 1 and 2 showed more significant changes in co-culture conditions than in single-cultured CMs while cluster 3 included genes that showed more significant changes in the CM-S condition and had few changes in the co-culture condition. This indicates that proteins in cluster 3 were most likely the ones that were stabilized by co-culturing with iECs, thus protecting CMs from oxidative stress.

Genes identified in these 3 clusters were searched against the STRING database to analyze the interaction probabilities among their protein products (Fig. 4). More complicated networks indicate higher possibility that genes within this cluster are working synergistically to affect cell functions. The accepted score threshold was set to be 0.9, which assured very high confidence for the results. Cluster 1 showed several STRING networks, including the fibroblast growth factors (*Fgf*) family genes, which were largely involved in angiogenesis, wound healing, and various endocrine signaling pathways; the potassium channels (*Kcn*) family genes, which could form potassium-selective pores that spanned cell membranes for signal transduction; and the *Wnt* family genes, which regulated cell-cell interactions during development and adult tissue homeostasis (Fig. 4A and Supplemental Table 5). With cluster 2, only limited gene interactions were identified, indicating that genes in cluster 2 performed biological functions as single proteins instead of as protein networks (Fig. 4B and Supplemental Table 6). The most interesting cluster we found was cluster 3, which showed highly interactive networks (Fig. 4C and Supplemental Table 7), indicating that these genes work highly interactively for regulating cellular responses. Because cluster 3 included genes that were upregulated in CM-S but not in CMEC-N or CMEC-S, the protein networks identified in cluster 3 were considered to be the ones that were stabilized by co-culturing with iECs in response to oxidative stress.

Some of these networks identified in cluster 3 included mitochondrial complex I [nicotinamide adenine dinucleotide (NADH) dehydrogenase (ubiquinone) (*Nduf*) subunits], mitochondrial complex IV (cytochrome *c* oxidase subunits), and mitochondrial complex V (ATP synthase subunits), three of the five protein complexes in the electron transport chain (ETC). Cluster 3 also contains the ribosomal protein complex. To understand the role of ETC complexes, the genes in mitochondrial complex I, III, IV, and V were extracted and visualized in heatmaps for their expressions under CM-S, CMEC-N and CMEC-S conditions (Fig. 5A–D and Supplemental Tables 8–12). Because the ETC complexes are present in the inner mitochondria membrane, the mitochondrial ribosomal protein (*Mrpl*) family was also analyzed (Fig. 5E). All these complexes showed similar trends that, under oxidative stress, the genes in these complexes were upregulated in single culture CMs, but were downregulated in CM-iEC co-culture condition without oxidative stress. In addition, we observed much less upregulation of these genes in CM-iEC co-culture condition under oxidative stress compared to CM-S, further proving the protective effects of iEC presence for CMs to resist damage from oxidative stress.

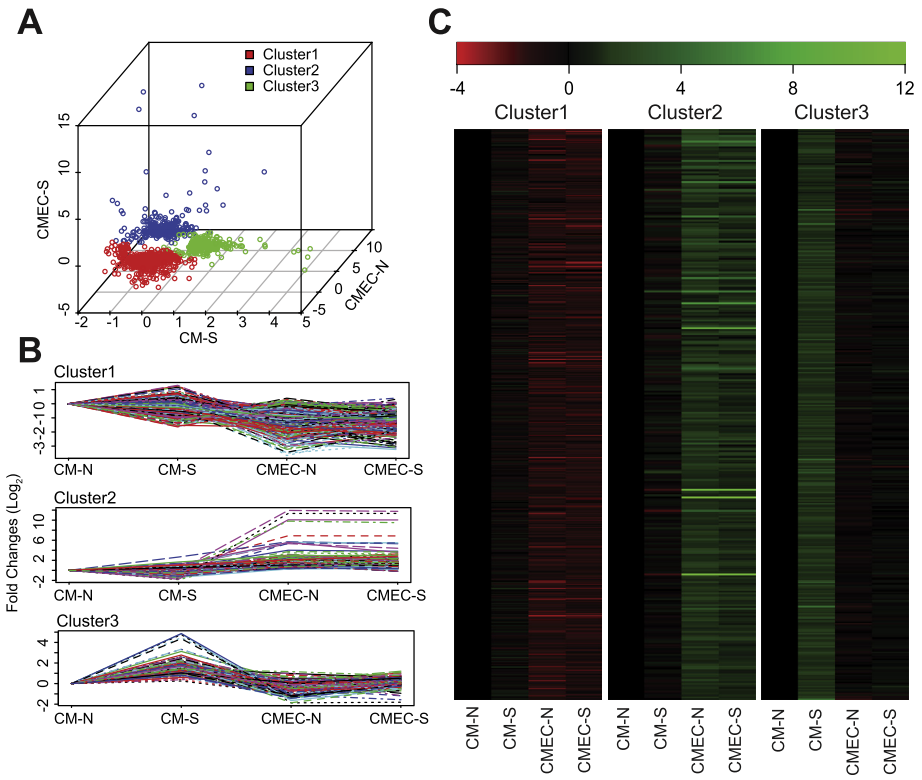

Fig. 3. Clustering of changed genes. A) Three clusters were identified with k-means classification algorithm. B) Expression trends of genes under CM-S, CMEC-N, and CMEC-S conditions in each cluster. Each line indicates the expression change of a single gene in the cluster. C) Heatmap of gene expression levels under CM-S, CMEC-N, and CMEC-S conditions in each cluster.

3.4. KEGG pathway analysis enriched different pathways in co-cultured and single cultured CMs under oxidative stress

KEGG pathway analysis is a useful tool for analyzing pathways involved in biological processes. The KEGG pathways were analyzed for their enrichment under CM-S, CMEC-N, and CMEC-S conditions, with significantly changed genes (p-value < 0.05, fold-change >2) in each condition (Fig. 6 and Supplemental Table 13). All gene expression levels were normalized to the corresponding expression levels in CM-N. The size of each circle indicates the gene ratio and the color indicates the score of the enrichment. The gene ratio is equal to the number of genes in the dataset that mapped to the pathway divided by total number of genes in the pathway. Higher gene ratio means more genes were identified in the sample sets for the pathway. The score indicates the association of the pathway to the experimental conditions. A higher score means stronger association and more confidence that the pathway is playing a role in the biological process.

One of the interesting pathways is the ribosome pathway, which was highly upregulated in CM-S but not in co-culture conditions, and the pathway showed a very high score (score 68.46, indicated by grey circle in Fig. 6 because it was too far above the score range) indicating a high confidence for its association with oxidative stress. However, the pathway was not enriched in the co-culture conditions regardless of exposure to oxidative stress or not. The activation of the ribosome pathway under oxidative stress is possibly a consequence of enhanced metabolic demands. In support of this, it was reported in the literature that ribosomal RNA synthesis was connected to cellular energy supply through the activation of AMP-activated protein kinase [34]. Another pathway that was enriched only in CM-S condition was the oxidative phosphorylation pathway. The oxidative phosphorylation pathway functions in oxidizing nutrients, and in releasing energy for reforming ATP. The enrichment of oxidative phosphorylation pathway in CM-S condition indicated the increased demand for energy supplies when CMs were under oxidative stress, as it is possibly needed to recover from damages due to the oxidative stress.

The genes identified in ribosome pathway were largely composed of *Mrpl* family genes, while the genes identified in oxidative phosphorylation pathway included genes in mitochondrial complexes I, IV, and V. The lack of enrichment for ribosome pathway and oxidative phosphorylation pathway in co-culture conditions agreed with the results from clustering and STRING analysis that the mitochondrial complexes and *Mrpl* family genes were upregulated in the CM-S condition but were stabilized in co-culture conditions.

The overall KEGG pathway analysis results showed that the CMEC-N condition enriched the largest number of KEGG pathways, although some of them contain few genes (with very low gene ratio). Some of these pathways that were enriched in the CMEC-N condition such as, *Rap1* signaling pathway, adrenergic signaling in cardiomyocytes, and the drug metabolism-cytochrome P450 pathway, were also enriched in the CMEC-S condition, indicating that the activation of these pathways in CMs through CM-iEC crosstalk could be crucial for cardioprotection under oxidative stress.

3.5. iECs co-cultured with CMs showed a stable gene expression profile in response to oxidative stress

The distribution of all genes identified in iECs showed that the gene expression fell in a Gaussian distribution centered at no expression changes, and most of the gene expression fell within 2-fold change range (Fig. 7A, grey bars). Within the 12,644 genes tested, only 160 genes were identified as significantly changed, showing expression level changes greater than 2-fold, and a

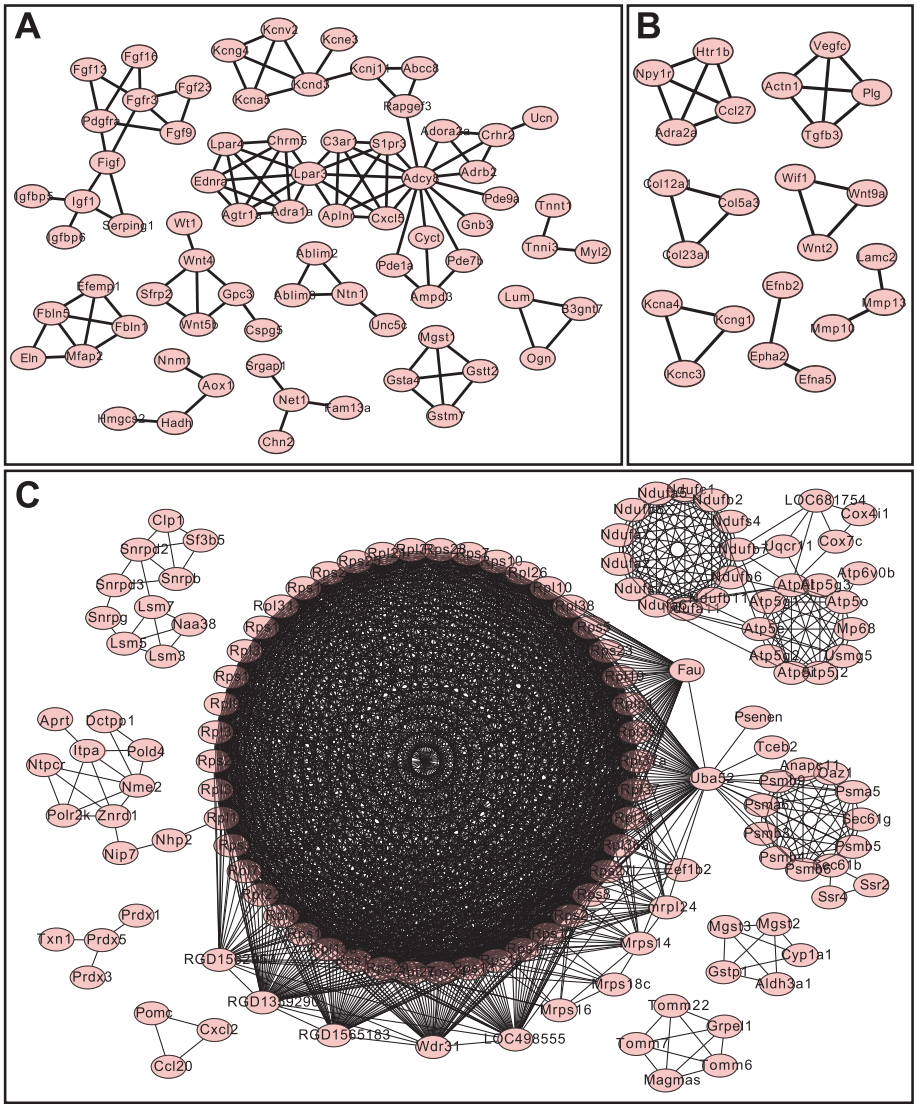

Fig. 4. Network analysis with STRING algorithm for A) Cluster 1, B) Cluster 2, and C) Cluster 3. The threshold of acceptable scores was set to be above 0.9. The details of protein interactions are listed in Supplemental Tables 5-7.

p-value less than 0.05 (Supplemental Table 14). Out of the 160 significantly changed genes, 80 were upregulated and 80 were downregulated (Fig. 7A, red bars; Fig. 7B, green dots). The STRING network analysis and KEGG pathway analysis failed to enrich meaningful pathways due to the limited amount of significantly changed genes (Fig. 7C). The very few and unobvious changes of gene profiles of iECs in co-culture with CMs in response to oxidative stress indicated that the CM-iEC interactions might have a stabilizing effect on iECs as well. It is also possible that the gene profile of iECs changed at an earlier time point, and at the time point we performed the transcriptome analysis the gene profile of iECs has already returned back to normal, thus we did not observe a drastic change in the gene profile of iECs under oxidative stress.

The most downregulated genes in response to oxidative stress in co-cultures included transmembrane protein 169 (*TMEM169*), kinase suppressor of ras 2 (*KSR2*), frizzled class receptor 5 (*FZD5*), and T-cell leukemia homeobox 1 (*TLX1*). Another interesting gene we found to be downregulated was HIF1A antisense RNA 1 (*HIF1A-AS1*). *HIF1A-AS1* had more than 4-fold downregulation in oxidative stress treated co-culture samples [33]. The most upregulated gene was dual specificity phosphatase 2 (*DUSP2*). It can dephosphorylate phosphoserine/threonine and phosphotyrosine residues, and regulate cellular proliferation and differentiation by negatively regulating members of the mitogen-activated protein kinase (MAPK) superfamily members such as MAPK/ERK, SAPK/JNK, and p38 [35]. The upregulation of *DUSP2* gene in iECs in CM-iEC co-culture condition under oxidative stress indicates that the protective effects of iECs on CMs might be a result of the suppression of MAPK pathways in iECs.

3.6. Data validation

There is a high-level protein homology between rats and humans in paracrine factors such as vascular endothelial growth factor (VEGF) [36]. To validate the *in vivo* relevance of the gene expression profile results we obtained using the engineered model tissue approach, we compared our CM gene expression profile data with a data set that was acquired using an *in vivo* rat MI model. The Gene Expression Omnibus (http://www.ncbi.nlm.nih.gov/geo) data series GSE4105 were chosen for validating our results, which compared gene expression profile of the ventricular tissue of a rat MI model 2 days after reperfusion (n = 3) to those of control rats (n = 3). Several genes that were reported to relate with oxidative stress were selected and extracted from GSE4105 data set to

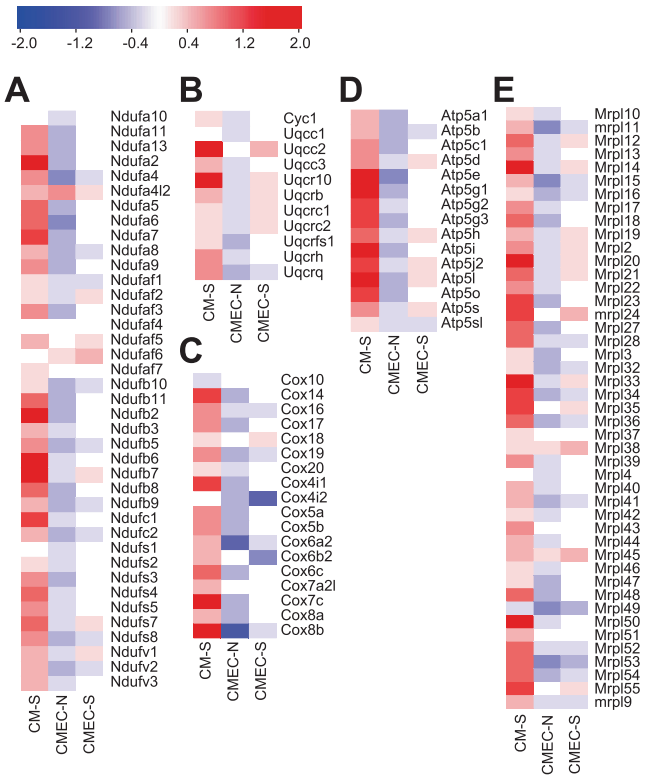

Fig. 5. Heatmap of gene expression under CM-S, CMEC-N, and CMEC-S conditions for A) mitochondrial complex I B) mitochondrial complex III, C) mitochondrial complex IV, D) mitochondrial complex V, and E) mitochondrial ribosomal protein complex.

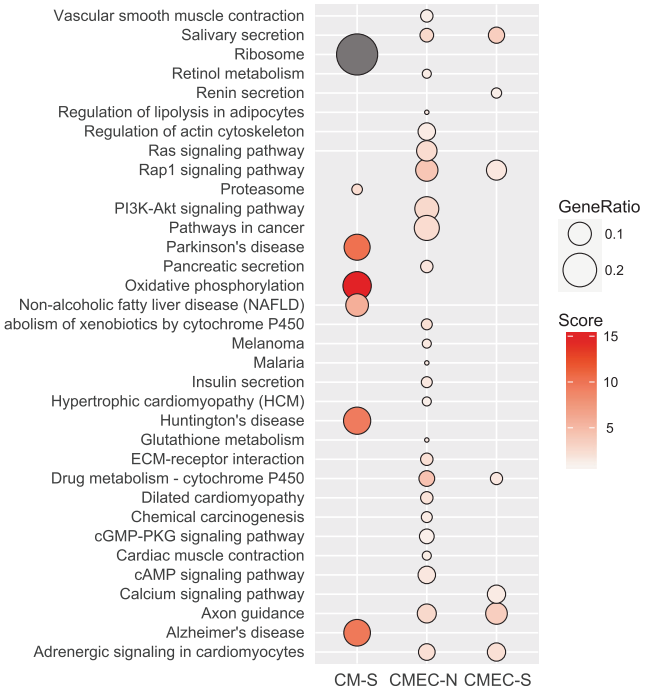

Fig. 6. KEGG pathway analysis showing enriched pathways under CM-S, CMEC-N, and CMEC-S conditions. Grey circle represent pathway with a score of 68.46.

compare with the CMEC-S versus CMEC-N results in this study. These genes include: 1) *Kcnk2*, also known as *Trek-1*, which is known to have protective effects on CHO cells treated with H_2O_2 [37]; 2) *Fmo1*, which is known to be activated by oxidative stress [38]; 3) *Mmp13*, which is a matrix metalloproteinase and gets activated in response to oxidative stress [39]; 4) *Aldh1l1*, which was reported to have increased expression in response to oxidative stress [40]; 5) *Mycn*, which was reported to be induced in cancer by oxidative stress, and helped to improve cancer cell survival [41]; and 6) *Gdf15*, which was induced during heart failure development and was elevated in MI patients [42]. The expression patterns of these genes in our result agree with the results reported in dataset GSE4105 (Fig. 8A). In addition, the cardiomyocyte-specific protein *Tnnt1* also showed an increase in expression in both our model tissues and in *in vivo* rat ventricles, under oxidative stress (Fig. 8B). The expression of these genes was shown in Fig. 8B.

To validate the changes in gene expression we observed in iECs, we used a clinical dataset GSE66360, which sequenced the transcriptome of circulating ECs isolated from MI patients (n = 49) or healthy people (n = 50). Specifically we looked into expression levels of *TMEM169* and *DUSP2* which showed the highest level of change, as well as *GIMAP6*, which is an endothelium specific gene [43], and *FANCF*, which was reported to be related to oxidative stress [44]. The result showed that in the clinical dataset GSE66360, the expression levels of *GIMAP6*, *FANCF, and TMEM169*, were downregulated by 0.35-fold, 0.47-fold, and 0.50-fold respectively in the MI patient circulating ECs, while *DUSP2* were upregulated by 1.88-fold in the MI patient circulating ECs (Fig. 8C). These findings are consistent with our results showing downregulation of *GIMAP6*, *FANCF*, and *TMEM169* by 0.30-fold, 0.48-fold, and 0.02-fold respectively, and upregulation of *DUSP2* by 8.66-fold in the iECs under oxidative stress condition (Fig. 8D). One thing to notice is that although *TMEM169* is downregulated while *DUSP2* is upregulated both in iECs under oxidative stress condition in tissue models and in MI patient circulating ECs, the changes in MI patients are less pronounced.

4. Discussion

Although the factors leading to MI are under intense study, endogenous cellular responses to MI that could preserve cell and organelle function are not well understood. One of the less investigated aspects of MI is CM-EC crosstalk and cardioprotection conferred by this crosstalk during MI. Studying the CM-EC crosstalk and endogenous cellular responses of CMs in animal models of MI is challenging due to high financial and time costs to generate and breed the animals, interference from other tissues, physiological differences between the animals and humans, and the inability to genetically alter different cells of a given tissue independently. Especially for studying the effect of paracrine factors, a tissue engineered human cardiac tissue would enable investigation of the CM-EC crosstalk in a high throughput and time-efficient manner and potentially avoid many of the disadvantages of an animal model.

In this study, we developed 3D engineered constructs to study the paracrine-only crosstalk between CMs and iECs under post-MI level oxidative stress. We made use of the properties of a synthetic polymer and made sure that the only interaction the cells had was through secreted factors, and that the cell-to-cell distance was kept the same throughout the course of the study. We performed detailed RNA-sequencing analysis on these 3D engineered models, with or without oxidative stress, and confirmed that the presence of iECs has a stabilizing effect on CMs' gene expression patterns under oxidative stress, supporting the improved CM survival under oxidative stress we observed in presence of iECs. A thorough analysis on global gene expression was performed to reveal the changes in CMs' response to oxidative stress in single culture or co-culture with iECs, as well as that of iECs' in the co-culture. Importantly, we analyzed the protein networks and

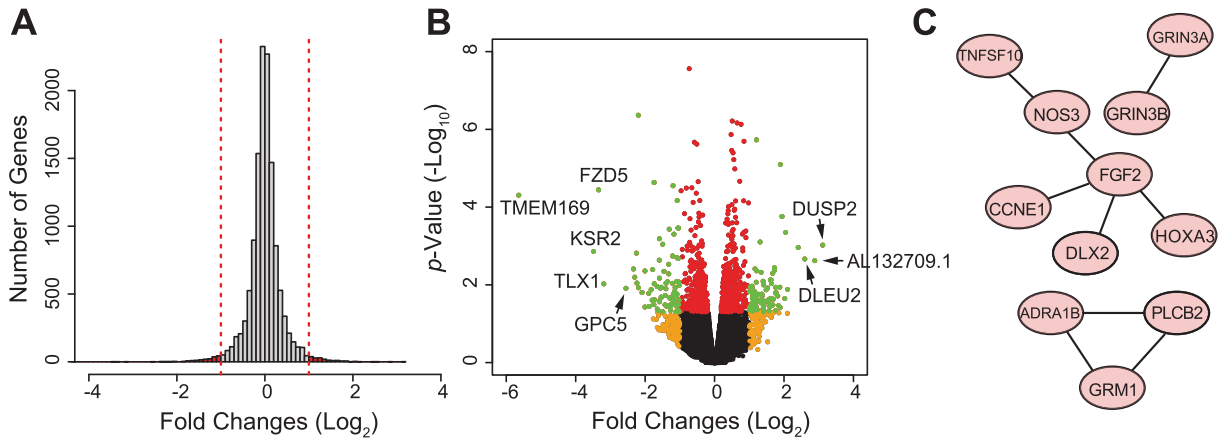

Fig. 7. Comparison of iECs under normal and oxidative stress conditions in co-culture with CMs. A) Distribution of gene expression level changes in CMEC-S. All gene expressions were normalized to iECs in CMEC-N condition. B) Volcano plot of gene expression changes in CMEC-S condition. Green dots show significantly changed genes. C) STRING networks of significantly changed genes in iECs under CMEC-S condition. All genes were screened with p-value < 0.05 and more than 2-fold expression changes.

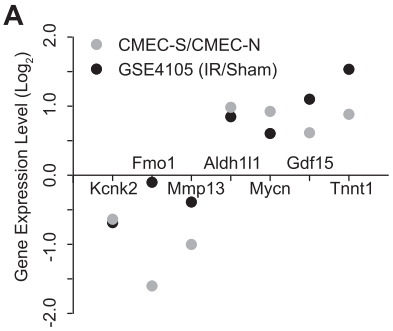

B

Gene	Fold Change (Log_2)	
	GSE4105 (IR/Sham)	CMEC-S/CMEC-N
Kcnk2	-0.68	-0.64
Fmo1	-0.10	-1.60
Mmp13	-0.39	-1.00
Aldh1l1	0.85	0.98
Mycn	0.60	0.92
Gdf15	1.10	0.61
Gdf15	1.53	0.88

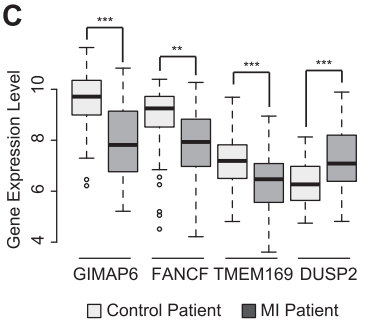

D

Gene	Fold Change*	p-Value
GIMAP6	0.30	9.37×10^{3}
FANCF	0.48	2.09×10^{3}
TMEM169	0.02	4.95×10^{5}
DUSP2	8.66	9.52×10^{4}

* Fold Change: the gene expression level in ECs in CMEC-S divided by the gene expression level in ECs in CMEC-N.

Fig. 8. Data validation and *in vivo* relevance of the engineered tissue model. A), B) Changes in the expression levels of *Kcnk2*, *Fmo1*, *Mmp13*, *Aldh1l1*, *Mycn*, *Gdf15*, and *Tnnt1* in GEO dataset GSE4105 and our dataset comparing oxidative stress conditions to normoxia conditions. C) Expression levels of *GIMAP6*, *FANCF*, *TMEM169*, and *DUSP2* in patients experiencing acute myocardial infarction (n = 49) and in healthy cohorts (n = 50). The gene expression levels are extracted from GEO dataset GSE66360. D) Changes in the gene expression levels of *GIMAP6*, *FANCF*, *TMEM169*, and *DUSP2* in iECs in CMEC-S compared to CMEC-N.

pathways that might take roles in protecting CMs from oxidative stress in the co-culture system.

The gene expression profiles of CMs showed drastic differences between single culture and co-culture samples when the CMEC-N condition was compared with CM-N, or CMEC-S condition was compared with CM-S. Several of these changed genes were related to oxidative stress, such as FYVE, RhoGEF and PH domain containing 5 (*Fgd5*), amphiregulin (*Areg*), secreted frizzled-related sequence protein 2 (*Sfrp2*), and NLR family, apoptosis inhibitory protein 6 (*Naip6*). FGD5 protein was reported to play a crucial role in vascular pruning processes, and to inhibit neovascularization [45]. AREG protein is a member of epidermal growth factor (EGF) family and was reported to have an increase in its expression when the cardiac tissue was loaded with mechanical stretch [46] and can promote cell proliferation through interaction with the EGF/TGF-α receptor. SFRP2 protein is a Wnt signal modulator and was reported to be a key paracrine factor, which was responsible for CM survival and repair after ischemic injury [47]. NAIP6 protein, also known as BIRC1 or NLRB1, is a component of the NLRC4 inflammasome (NLRC4 stands for NLR family CARD domain-containing protein 4), and is an *anti*-apoptotic protein whose dysregulation is associated with spinal muscle atrophy [48,49]. The NLR inflammasomes were reported to be able to protect CMs [50] from apoptosis caused by ischemic injury. In the CM-iEC co-culture models, both *Fgd5* and *Sfrp2* were downregulated, indicating less apoptosis in the co-culture condition, while *Areg* and *Naip6* was upregulated, indicating improved survival in the co-culture condition.

A recent study by Clerk et al. analyzed the global gene expression changes of rat CMs in response to H_2O_2 in 2D single culture conditions [51], and they reported 644 genes changed their expression levels at different time points after oxidative stress challenge.

These 644 genes were compared with the genes we identified in 3D biomimetic CM-only cell cultures (CM-S), and 494 genes were found to be overlapping between the 2D and 3D culture systems, but with very different expression levels (Supplemental Tables 15–19). One interesting gene is *Slc2a4*, also known as *Glut4,* the expression of which decreased 0.44-fold in 2D CM cultures but increased 1.80-fold in 3D CM cultures in response to oxidative stress. Glut4 is associated with diabetes and its mRNA expression decreases after 4 h of exposure to H_2O_2 in 3T3-L1 adipocytes [52]. It was previously reported that *Glut4* was a target of miR-223 and miR-223 induced *Glut4* upregulation was necessary and sufficient for the increase of glucose uptake in neonatal rat ventricular myocytes [53]. In the mature heart, GLUT4 is mainly present in intracellular membrane compartments, and it translocates to the cell membrane in response to stimuli such as hypoxia/ischemia or insulin, thus enhancing glucose uptake in cardiomyocytes to overcome the stress [54,55]. The downregulation of *Glut4* in 2D but upregulation in 3D when treated with oxidative stress indicates that the 3D hydrogel cultures are providing a model that better represents the *in vivo* mouse/rat model. Interestingly, in the CM-iEC co-culture tissue models the increase of *Glut4* was not observed in response to oxidative stress, consistent with our other results indicating the protective effect of iECs on CMs.

Another interesting gene is Fos-like antigen 1 (*Fosl1*), also known as *Fra1*, which increased 2.92-fold in 2D CM cultures but decreased 0.74-fold in 3D CM cultures. *Fra1* is a component of activator protein 1 (AP-1) which is composed of dimeric basic region-leucine zipper (bZIP) proteins including JUN, FOS, MAF and ATF sub-family members [56]. It was shown that higher AP-1 activity correlated with resistance to oxidative stress in myoblasts [57]. Bergman et al. reported that neonatal rat cardiac fibroblasts cultured under hypoxia conditions with 1% oxygen for 24 h showed increased AP-1 activity which led to enhanced matrix metalloproteinase 2 (*Mmp2*) transcription for more than 5-fold enhancement of MMP2 synthesis, which was one of the major mediators of ventricular dysfunction or fibrosis [58]. This increase of AP-1 activity is due to the shift from binding with JUNB-FRA1 heterodimer under normoxic conditions, and binding with JUNB-FOSB heterodimer under hypoxic conditions [58]. Venugopal et al. showed similar results where upregulation of *Fra1* expression repressed human antioxidant response element (hARE), which is composed of two AP-1 elements [59]. hARE is required for high basal transcription of the NAD(P)H:quinone oxidoreductase 1 (*Nqo1*) gene as well as its induction in response to antioxidants. NQO1 catalyzes reductive detoxification of quinones and its derivatives thus can protect cells against oxidative stress [59]. In other words, upregulation of *Fra-1* will repress hARE thus repress *Nqo1* transcription, which will inhibit protection against oxidative stress. The upregulation of *Fra1* in 2D-cultured CMs but downregulation in 3D-cultured CMs indicates CMs in 3D cultures are protected from oxidative stress compared to those in 2D cultures. Moreover, although CMEC-N showed 1.5-fold higher expression of *Fra1* compared to CM-N, under oxidative stress the expression level of *Fra1* decreased by 0.35-fold in co-cultured CMs, compared to the decrease by 0.27-fold in 3D single cultured CMs, further providing the iEC-driven protection of CMs in response to oxidative stress.

KEGG pathway analysis showed that the oxidative phosphorylation pathway was significantly enriched solely in the CM-S group. The results show that one group of genes that showed a drastic change in expression were mitochondrial complex I, the first and the largest protein complex of the electron transport chain (ETC) [60], along with the other complexes of ETC. It was previously shown that a reduction in mitochondrial complex I enzymatic activity was detected in mitochondria isolated from heart failure model of adult mongrel dogs' CMs [61] as opposed to the increased expression levels we observed here. This may be a result of functional uncoupling of the respiratory chain in heart failure mitochondria due to the long-term (4-weeks) treatment with rapid ventricular pacing at 240 bpm for generating the animal model, as compared to the treatment time of 16 h in our research. On the other hand, this upregulation in oxidative phosphorylation is in parallel with the cells' response to various drugs [62]. Wagner et al., have screened 2,490 drugs and investigated the effect of these drugs on expression of ETC proteins transcribed by both mitochondrial and nuclear DNA of murine muscle cells cultured in 2D [62]. They reported that most of these drugs induced an upregulation in both mitochondrial and nuclear DNA transcripts, similar to the correlated upregulation induced by oxidative stress we observe in this study. We can clearly observe the stabilizing effect of iECs on CM metabolism under oxidative stress. The fact that we do not observe any significant change in the energy metabolism of the cells in the co-culture condition, in normoxia or oxidative stress, would support the possible need for the increased metabolism of CMs in the absence of iECs.

Another enriched pathway was the drug metabolism-cytochrome P450 pathway. We observed that this pathway was mostly enriched in the co-culture conditions. Exploring the enriched genes in this pathway in more detail, we found that Glutathione-S-Transferases (*Gst*), namely the *Gsta1*, *Gsta4*, and *Gsta5* were downregulated in the co-culture conditions with or without stress, yet there was no change in the expression of *Gsta4* and *Gsta5*, and *Gsta1* was upregulated only in CM-S condition. GSTs are enzymes that inactivate the electrophilic compounds and toxic substrates, thus serving as intracellular antioxidants [63,64]. The specific role of GSTs in CMs under ischemia/reperfusion (I/R) induced oxidative stress was studied by Roth et al. They have shown that the inhibition of GST in isolated neonatal rat CMs, cultured in a conventional 2D culture system, leads to an increase in apoptosis [65]. In addition, they observed that this effect is more drastic if they expose the CMs to I/R and inhibit GST activity. The significantly lower expression of GSTs in co-culture conditions we observed in this study suggests that in the presence of iECs the CMs do not activate the antioxidant pathways. Especially the upregulation of *Gsta1* in CM-S condition indicates that when cultured alone, CMs activate the GST pathways in order to protect themselves against the oxidative damage caused by the stress applied. Similarly, associated with the same pathway, Flavin containing monooxygenases (*Fmo*); *Fmo1*, *Fmo2*, and *Fmo4* were downregulated in co-culture conditions compared to CMs alone, with or without oxidative stress. FMO family proteins catalyze the oxygenation of nucleophilic molecules and have similar characteristics to cytochrome P450 enzymes, detoxifying drugs and xenobiotics [66]. Kim et al. showed that the expression of *Fmo1* was increased significantly in the cardiac tissues of patients with atrial fibrillation, which is a condition that results due to oxidative stress [38]. This result was supported by the downregulation of *Fmo* genes we observed in our co-culture systems. This result is also in parallel with the expression changes in *Gsta* genes and overall suggests that CMs alone trigger oxygen radical detoxifying mechanisms in the cell.

Excess levels of reactive oxygen species (ROS), such as H_2O_2, were observed in pathological conditions and could promote apoptosis and affect neovascularization in iECs [67]. It was reported that relatively high concentrations of H_2O_2 (>0.2 mM) could activate PKC, small G protein Rho, and Src tyrosine kinase, which has been shown to lead to increased endothelial permeability [68]. Treatment with 0.1 mM of H_2O_2 was shown to induce apoptosis of HUVECs, which was inhibited by pre-incubation with resveratrol, which enhanced the antioxidant defenses, and inhibited the mitochondrial membrane potential digression [69]. In this study, the transcriptome of 3D single cultured iECs under oxidative stress was not analyzed. However, it is expected that 0.2 mM of H_2O_2

treatment would cause gene profile changes in 3D single cultured iECs. The gene profiles did not show much change with or without 0.2 mM of H_2O_2 treatment for iECs when co-cultured with CMs, which could suggest potential protective effects of CMs on iECs that stabilized their gene expression in response to oxidative stress. Another possibility is that the gene profile changes of the iECs occur quickly, causing them to release cardioprotective factors at an earlier time point. These factors then stabilize or activate genes in the CMs and protect them under oxidative stress. At the 18 h time point (16 h of H_2O_2 treatment followed by 2 h of recovery), the gene profile of the iECs could have already returned back to untreated level. Previous reports show that the gene profile of ECs can change within very short period. HUVECs treated with 100 μM of homocysteine showed expression changes of NFkB within 2 h [70], and with VEGF treatment, ECs showed complicated gene profile changes as fast as after 30 min, with large amount of genes' expression level peaked at 30 min, 2 h, or 6 h, which returned to the expression level of untreated ECs at 24 h [71]. The third possibility is that the factors originating from the iECs that conferred gene expression stability to the CMs are controlled post-transcriptionally or act at the protein level. In fact, one of the most interesting genes we found to be downregulated was *HIF1A-AS1* which is a recently identified non-coding RNA that downregulates hypoxia inducible factor 1-α (*HIF1A*) post-transcriptionally. *HIF1A-AS1* expression was downregulated more than 4-fold in iECs that were co-cultured with CMs under oxidative stress [33]. To fully understand effects of oxidative stress on iECs, analysis of iEC-only cultures as well as time-lapse measurements would be required.

5. Conclusions

In conclusion, 3D biomimetic engineered tissues studied here allowed us to distinguish between the gene expression profile changes of CMs versus iECs, while being able to focus on paracrine-only effects in these two cell types' crosstalk. CM-iEC co-cultures showed different gene expression profiles compared to CM single cultures, and these expression profiles in CM-iEC co-cultures were preserved under oxidative stress. We observed that the iECs had a stabilizing effect over the global gene expression profile of CMs under oxidative stress. Moreover, our results show that the protecting effect was mediated by stabilizing CM ribosomal and mitochondria complexes, altering gene expressions in CMs related to apoptosis, proliferation, and by suppressing oxidative phosphorylation pathway while activating pathways such as drug metabolism-cytochrome P450 pathway, *Rap1* signaling pathway, and adrenergic signaling in cardiomyocytes pathway. Finally, our results prove the *in vivo* as well as clinical relevance of 3D biomimetic synthetic tissues as disease models, as shown by the correlating gene expression patterns we observed when we compared our data with available *in vivo* and clinical data sets. Data presented in this study could lead to identification of target pathways or molecules in CM-iEC communication in the aftermath of MI, and could help to reveal the mechanisms of iECs' protective effects on CMs under stress conditions.

Disclosure

No conflict of interest is declared.

Acknowledgments

We thank Dr. C. Cowan, Dr. K. Musunuru, and Dr. L. Challet-Meylan, Harvard University, for providing human induced pluripotent cells and reagents, and for their helpful suggestions and scientific insight on stem cell culture and differentiation. This publication was supported by a Project Development Team within the ICTSI NIH/NCRR [Grant Number UL1TR001108], and NSF CBET CAREER Award [Grant Number 1651385].

Appendix A. Supplementary data

Supplementary data associated with this article can be found, in the online version, at http://dx.doi.org/10.1016/j.actbio.2017.06.031.

References

[1] E.A. Liehn, O. Postea, A. Curaj, N. Marx, Repair after myocardial infarction, between fantasy and reality: the role of chemokines, J. Am. Coll. Cardiol. 58 (2011) 2357–2362.
[2] M. Abrial, C.C. Da Silva, B. Pillot, L. Augeul, F. Ivanes, G. Teixeira, R. Cartier, D. Angoulvant, M. Ovize, R. Ferrera, Cardiac fibroblasts protect cardiomyocytes against lethal ischemia-reperfusion injury, J. Mol. Cell Cardiol. 68 (2014) 56–65.
[3] E. Ongstad, P. Kohl, Fibroblast-myocyte coupling in the heart: potential relevance for therapeutic interventions, J. Mol. Cell. Cardiol. 91 (2016) 238–246.
[4] T.M. Leucker, M. Bienengraeber, M. Muravyeva, I. Baotic, D. Weihrauch, A.K. Brzezinska, D.C. Warltier, J.R. Kersten, P.F. Jr, Pratt, Endothelial-cardiomyocyte crosstalk enhances pharmacological cardioprotection, J. Mol. Cell. Cardiol. 51 (2011) 803–811.
[5] R.F. Furchgott, J.V. Zawadzki, The obligatory role of endothelial cells in the relaxation of arterial smooth muscle by acetylcholine, Nature 288 (1980) 373–376.
[6] J. Noireaud, R. Andriantsitohaina, Recent insights in the paracrine modulation of cardiomyocyte contractility by cardiac endothelial cells, BioMed. Res. Int. 2014 (2014) 923805.
[7] Y. Arita, Y. Nakaoka, T. Matsunaga, H. Kidoya, K. Yamamizu, Y. Arima, T. Kataoka-Hashimoto, K. Ikeoka, T. Yasui, T. Masaki, K. Yamamoto, K. Higuchi, J.S. Park, M. Shirai, K. Nishiyama, H. Yamagishi, K. Otsu, H. Kurihara, T. Minami, K. Yamauchi-Takihara, G.Y. Koh, N. Mochizuki, N. Takakura, Y. Sakata, J.K. Yamashita, I. Komuro, Myocardium-derived angiopoietin-1 is essential for coronary vein formation in the developing heart, Nat. Commun. 5 (2014) 4552.
[8] Y. Tian, E.E. Morrisey, Importance of myocyte-nonmyocyte interactions in cardiac development and disease, Circ. Res. 110 (2012) 1023–1034.
[9] O. Cleaver, D.A. Melton, Endothelial signaling during development, Nat. Med. 9 (2003) 661–668.
[10] F.M. Drawnel, C.R. Archer, H.L. Roderick, The role of the paracrine/autocrine mediator endothelin-1 in regulation of cardiac contractility and growth, Br. J. Pharmacol. 168 (2013) 296–317.
[11] B. Wu, Z. Zhang, W. Lui, X. Chen, Y. Wang, A. Chamberlain, R.A. Moreno-Rodriquez, R.R. Markwald, B.P. O'Rourke, D.J. Sharp, D. Zheng, J. Lenz, H.S. Baldwin, C.P. Chang, B. Zhou, Endocardial cells form the coronary arteries by angiogenesis through myocardial-endocardial VEGF signaling, Cell 151 (2012) 1083–1096.
[12] K.H. Park, W.J. Park, Endothelial dysfunction: clinical implications in cardiovascular disease and therapeutic approaches, J. Korean Med. Sci. 30 (2015) 1213–1225.
[13] G. Favero, C. Paganelli, B. Buffoli, L.F. Rodella, R. Rezzani, Endothelium and its alterations in cardiovascular diseases: life style intervention, BioMed, Res. Int. 2014 (2014) 801896.
[14] T.M. Leucker, Z.D. Ge, J. Procknow, Y. Liu, Y. Shi, M. Bienengraeber, D.C. Warltier, J.R. Kersten, Impairment of endothelial-myocardial interaction increases the susceptibility of cardiomyocytes to ischemia/reperfusion injury, PLoS One 8 (2013) e70088.
[15] P. Dowling, M. Clynes, Conditioned media from cell lines: a complementary model to clinical specimens for the discovery of disease-specific biomarkers, Proteomics 11 (2011) 794–804.
[16] T.S. Hakim, K. Sugimori, E.M. Camporesi, G. Anderson, Half-life of nitric oxide in aqueous solutions with and without haemoglobin, Physiol. Meas. 17 (1996) 267–277.
[17] F. Rodríguez-Pascual, O. Busnadiego, J. González-Santamaría, The profibrotic role of endothelin-1: is the door still open for the treatment of fibrotic diseases?, Life Sci 118 (2014) 156–164.
[18] X. Liu, X. Gu, Z. Li, X. Li, H. Li, J. Chang, P. Chen, J. Jin, B. Xi, D. Chen, D. Lai, R.M. Graham, M. Zhou, Neuregulin-1/erbB-activation improves cardiac function and survival in models of ischemic, dilated, and viral cardiomyopathy, J. Am. Coll. Cardiol. 48 (2006) 1438–1447.
[19] H.F. Lu, M. Leong, T. Lim, Y.P. Chua, J.K. Lim, C. Du, A.C. Wan, Engineering a functional three-dimensional human cardiac tissue model for drug toxicity screening, Biofabrication (2017), http://dx.doi.org/10.1088/1758-5090/aa6c3a [ahead of print].
[20] G. Wang, M.L. McCain, L. Yang, A. He, F.S. Pasqualini, A. Agarwal, H. Yuan, D. Jiang, D. Zhang, L. Zangi, J.G.A.E. Roberts, Q. Ma, J. Ding, J. Chen, D. Wang, K.L.J. Wang, R.J.A. Wanders, W. Kulik, F.M. Vaz, M.A. Laflamme, C.E. Murry, K.R. Chien, R.I. Kelley, G.M. Church, K.K. Parker, W.T. Pu, Modeling the

mitochondrial cardiomyopathy of Barth syndrome with induced pluripotent stem cell and heart-on-chip technologies, Nat. Med. 20 (2014) 616–623.
[21] D.R. Bayzigitov, S.P. Medvedev, E.V. Dementyeva, S.A. Bayramova, E.A. Pokushalov, A.M. Karaskov, S.M. Zakian, Human induced pluripotent stem cell-derived cardiomyocytes afford new opportunities in inherited cardiovascular disease modeling, Cardiol. Res. Pract. (2016) 3582380.
[22] B.W. Ellis, A. Acun, U.I. Can, P. Zorlutuna, Human iPSC-derived myocardium-on-chip with capillary-like flow for personalized medicine, Biomicrofluidics 11 (2017) 024105.
[23] S.P. Sheehy, F. Pasqualini, A. Grosberg, S.J. Park, Y. Aratyn-Schaus, K.K. Parker, Quality metrics for stem cell-derived cardiac myocytes, Stem Cell Rep. 2 (2014) 282–294.
[24] G.J. Wang, L.Y. Guo, H.X. Wang, Y.S. Yao, IP3R and RyR calcium channels are involved in neonatal rat cardiac myocyte hypertrophy induced by tumor necrosis factor-α, Am. J. Transl. Res. 9 (2017) 343–354.
[25] Rat Genome Sequencing Project Consortium, Genome sequence of the Brown Norway rat yields insights into mammalian evolution, Nature 428 (2004) 493–521.
[26] M. Tanaka, H. Ito, S. Adachi, H. Akimoto, T. Nishikawa, T. Kasajima, F. Marumo, M. Hiroe, Hypoxia induces apoptosis with enhanced expression of Fas antigen messenger RNA in cultured neonatal rat cardiomyocytes, Circ. Res. 75 (1994) 426–433.
[27] C. Patsch, L. Challet-Meylan, E.C. Thoma, E. Urich, T. Heckel, J.F. O'Sullivan, S.J. Grainger, F.G. Kapp, L. Sun, K. Christensen, Y. Xia, M.H. Florido, W. He, W. Pan, M. Prummer, C.R. Warren, R. Jakob-Roetne, U. Certa, R. Jagasia, P.O. Freskgård, I. Adatto, D. Kling, P. Huang, L.I. Zon, E.L. Chaikof, R.E. Gerszten, M. Graf, R. Iacone, C.A. Cowan, Generation of vascular endothelial and smooth muscle cells from human pluripotent stem cells, Nat. Cell Biol. 17 (2015) 994–1003.
[28] H. Merwald, G. Klosner, C. Kokesch, M. Der-Petrossian, H. Honigsmann, F. Trautinger, UVA-induced oxidative damage and cytotoxicity depend on the mode of exposure, J. Photochem. Photobiol. B 79 (2005) 197–207.
[29] J. Shorrocks, N.D. Paul, T.J. McMillan, The dose rate of UVA treatment influences the cellular response of HaCaT keratinocytes, J. Invest. Dermatol. 128 (2008) 685–693.
[30] G. Yu, L. Wang, Y. Han, Q. He, clusterProfiler: an R package for comparing biological themes among gene clusters, OMICS 16 (2012) 284–287.
[31] A. Franceschini, D. Szklarczyk, S. Frankild, M. Kuhn, M. Simonovic, A. Roth, J. Lin, P. Minguez, P. Bork, C. von Mering, L.J. Jensen, STRING v9.1: protein-protein interaction networks, with increased coverage and integration, Nucl. Acids. Res. 41 (Database issue) (2013) D808–D815.
[32] A.J. Engler, C. Carag-Krieger, C.P. Johnson, M. Raab, H.Y. Tang, D.W. Speicher, J. W. Sanger, J.M. Sanger, D.E. Discher, Embryonic cardiomyocytes beat best on a matrix with heart-like elasticity: scar-like rigidity inhibits beating, J. Cell. Sci. 121 (2008) 3794–3802.
[33] A. Acun, P. Zorlutuna, Engineered myocardium model to study the roles of HIF-1α and HIF1A-AS1 in paracrine-only signaling under pathological level oxidative stress, Acta Biomater. 58 (2017) 323–336.
[34] S. Hoppe, H. Bierhoff, I. Cado, A. Weber, M. Tiebe, I. Grummt, R. Voit, AMP-activated protein kinase adapts rRNA synthesis to cellular energy supply, Proc. Natl. Acad. Sci. U.S.A. 106 (2009) 17781–17786.
[35] D.M. Owens, S.M. Keyse, Differential regulation of MAP kinase signalling by dual-specificity protein phosphatases, Oncogene 26 (2007) 3203–3213.
[36] S. Kashida, N. Sugino, S. Takiguchi, A. Karube, H. Takayama, Y. Yamagata, Y. Nakamura, H. Kato, Regulation and role of vascular endothelial growth factor in the corpus luteum during mid-pregnancy in rats, Biol Reprod. 64 (2001) 317–323.
[37] L.N. Sun, L.L. Li, Z.B. Li, L. Wang, X.L. Wang, Protective effects of TREK-1 against oxidative injury induced by SNP and H_2O_2, Acta. Pharmacol. Sin. 29 (2008) 1150–1156.
[38] Y.H. Kim, D.S. Lim, J.H. Lee, W.J. Shim, Y.M. Ro, G.H. Park, K.G. Becker, Y.S. Cho-Chung, M.K. Kim, Gene expression profiling of oxidative stress on atrial fibrillation in humans, Exp. Mol. Med. 35 (2003) 336–349.
[39] D.A. Siwik, P.J. Pagano, W.S. Colucci, Oxidative stress regulates collagen synthesis and matrix metalloproteinase activity in cardiac fibroblasts, Am. J. Physiol. Cell Physiol. 280 (2001) C53–60.
[40] V. Vasiliou, D.W. Nebert, Analysis and update of the human aldehyde dehydrogenase (ALDH) gene family, Hum. Genomics 2 (2005) 138–143.
[41] S.S. Cao, R.J. Kaufman, Endoplasmic reticulum stress and oxidative stress in cell fate decision and human disease, Antioxid. Redox. Signal 21 (2014) 396–413.
[42] A. Dominguez-Rodriguez, P. Abreu-Gonzalez, P. Avanzas, Relation of growth-differentiation factor 15 to left ventricular remodeling in ST-segment elevation myocardial infarction, Am. J. Cardiol. 108 (2011) 955–958.
[43] M. Bhasin, L. Yuan, D.B. Keskin, H.H. Otu, T.A. Libermann, P. Oettgen, Bioinformatic identification and characterization of human endothelial cell-restricted genes, BMC Genomics 11 (2010) 342.
[44] R. Rani, J. Li, Q. Pang, Differential p53 engagement in response to oxidative and oncogenic stresses in Fanconi anemia mice, Cancer Res. 68 (2008) 9693–9702.
[45] C. Cheng, R. Haasdijk, D. Tempel, E.H. van de Kamp, R. Herpers, F. Bos, W.K. Den Dekker, L.A. Blonden, R. de Jong, P.E. Bürgisser, I. Chrifi, E.A. Biessen, S. Dimmeler, S. Schulte-Merker, H.J. Duckers, Endothelial cell-specific FGD5 involvement in vascular pruning defines neovessel fate in mice, Circulation 125 (2012) 3142–3158.
[46] F. Ye, F. Yuan, X. Li, N. Cooper, J.P. Tinney, B.B. Keller, Gene expression profiles in engineered cardiac tissues respond to mechanical loading and inhibition of tyrosine kinases, Physiol. Rep. 1 (2013) e00078.
[47] M. Mirotsou, Z. Zhang, A. Deb, L. Zhang, M. Gnecchi, N. Noiseux, H. Mu, A. Pachori, V. Dzau, Secreted frizzled related protein 2 (Sfrp2) is the key Akt-mesenchymal stem cell-released paracrine factor mediating myocardial survival and repair, Proc. Natl. Acad. Sci. U.S.A. 104 (2007) 1643–1648.
[48] S.L. Lage, C. Longo, L.M. Branco, T.B. da Costa, L. Buzzo Cde, K.R. Bortoluci, Emerging concepts about NAIP/NLRC4 inflammasomes, Front. Immunol. 5 (2014) 309.
[49] R. Götz, C. Karch, M.R. Digby, J. Troppmair, U.R. Rapp, M. Sendtner, The neuronal apoptosis inhibitory protein suppresses neuronal differentiation and apoptosis in PC12 cells, Hum. Mol. Genet. 9 (2000) 2479–2489.
[50] L. Lin, A.A. Knowlton, Innate immunity and cardiomyocytes in ischemic heart disease, Life Sci. 100 (2014) 1–8.
[51] A. Clerk, T.J. Kemp, G. Zoumpoulidou, P.H. Sugden, Cardiac myocyte gene expression profiling during H_2O_2-induced apoptosis, Physiol. Genomics 29 (2007) 118–127.
[52] D. Pessler, A. Rudich, N. Bashan, Oxidative stress impairs nuclear proteins binding to the insulin responsive element in the GLUT4 promoter, Diabetologia 44 (2001) 2156–2164.
[53] H. Lu, R.J. Buchan, S.A. Cook, MicroRNA-223 regulates Glut4 expression and cardiomyocyte glucose metabolism, Cardiovasc. Res. 86 (2010) 410–420.
[54] C. Montessuit, R. Lerch, Regulation and dysregulation of glucose transport in cardiomyocytes, Biochim. Biophys. Acta 2013 (1833) 848–856.
[55] T. Horie, K. Ono, K. Nagao, H. Nishi, M. Kinoshita, T. Kawamura, H. Wada, A. Shimatsu, T. Kita, K. Hasegawa, Oxidative stress induces GLUT4 translocation by activation of PI3-K/Akt and dual AMPK kinase in cardiac myocytes, J. Cell Physiol. 215 (2008) 733–742.
[56] N. Selvaraj, J.A. Budka, M.W. Ferris, J.P. Plotnik, P.C. Hollenhorst, Extracellular signal-regulated kinase signaling regulates the opposing roles of JUN family transcription factors at ETS/AP-1 sites and in cell migration, Mol. Cell. Biol. 35 (2015) 88–100.
[57] M.V. Catani, I. Savini, G. Duranti, D. Caporossi, R. Ceci, S. Sabatini, L. Avigliano, Nuclear factor kappaB and activating protein 1 are involved in differentiation-related resistance to oxidative stress in skeletal muscle cells, Free Radic. Biol. Med. 37 (2004) 1024–1036.
[58] M.R. Bergman, S. Cheng, N. Honbo, L. Piacentini, J.S. Karliner, D.H. Lovett, A functional activating protein 1 (AP-1) site regulates matrix metalloproteinase 2 (MMP-2) transcription by cardiac cells through interactions with JunB-Fra1 and JunB-FosB heterodimers, Biochem. J. 369 (2003) 485–496.
[59] R. Venugopal, A.K. Jaiswal, Nrf1 and Nrf2 positively and c-Fos and Fra1 negatively regulate the human antioxidant response element-mediated expression of NAD(P)H: quinone oxidoreductase1 gene, Proc. Natl. Acad. Sci. U.S.A. 93 (1996) 14960–14965.
[60] G. Beutner, R.A. Eliseev, G.A. Porter, Initiation of electron transport chain activity in the embryonic heart coincides with the activation of mitochondrial complex 1 and the formation of supercomplexes, PLoS One 9 (2014) e113330.
[61] T. Ide, H. Tsutsui, S. Kinugawa, H. Utsumi, D. Kang, N. Hattori, K. Uchida, Arimura Ki, K. Egashira, A. Takeshita, Mitochondrial electron transport complex I is a potential source of oxygen free radicals in the failingmyocardium, Circ. Res. 85 (1999) 357–363.
[62] B.K. Wagner, T. Kitami, T.J. Gilbert, D. Peck, A. Ramanathan, S.L. Schreiber, T.R. Golub, V.K. Mootha, Large-scale chemical dissection of mitochondrial function, Nat. Biotechnol. 26 (2008) 343–351.
[63] S.S. Singhal, S.P. Singh, P. Singhal, D. Horne, J. Singhal, S. Awasthi, Antioxidant role of Glutathione S-Transferases: 4-Hydroxynonenal, a key molecule in stress-mediated signaling, Toxicol. Appl. Pharmacol. 289 (2015) 361–370.
[64] A. Klaus, S. Zorman, A. Berthier, C. Polge, S. Ramirez, S. Michelland, M. Sève, D. Vertommen, M. Rider, N. Lentze, D. Auerbach, U. Schlattner, Glutathione S-Transferases interact with AMP-activated protein kinase: evidence for S-Glutathionylation and activation in vitro, PLoS One 8 (2013) e62497.
[65] E. Röth, N. Marczin, B. Balatonyi, S. Ghosh, V. Kovács, N. Alotti, B. Borsiczky, B. Gasz, Effect of a glutathione S-transferase inhibitor on oxidative stress and ischemia-reperfusion-induced apoptotic signaling of cultured cardiomyocytes, Exp. Clin. Cardiol. 16 (2011) 92–96.
[66] S.K. Krueger, D.E. Williams, Mammalian flavin-containing monooxygenases: structure/function, genetic polymorphisms and role in drug metabolism, Pharmacol. Ther. 106 (2005) 357–387.
[67] T.G. Ebrahimian, C. Heymes, D. You, O. Blanc-Brude, B. Mees, L. Waeckel, M. Duriez, J. Vilar, R.P. Brandes, B.I. Levy, A.M. Shah, J.S. Silvestre, NADPH oxidase-derived overproduction of reactive oxygen species impairs postischemic neovascularization in mice with type 1 diabetes, Am. J. Pathol. 169 (2006) 719–728.
[68] H. Cai, Hydrogen peroxide regulation of endothelial function: origins, mechanisms, and consequences, Cardiovasc. Res. 68 (2005) 26–36.
[69] L. Liu, L. Gu, Q. Ma, D. Zhu, X. Huang, Resveratrol attenuates hydrogen peroxide-induced apoptosis in human umbilical vein endothelial cells, Eur. Rev. Med. Pharmacol. Sci. 17 (2013) 88–94.
[70] R. Foncea, C. Carvajal, C. Almarza, F. Leighton, Endothelial cell oxidative stress and signal transduction, Biol. Res. 33 (2000) 89–96.
[71] M. Abe, Y. Sato, cDNA microarray analysis of the gene expression profile of VEGF-activated human umbilical vein endothelial cells, Angiogenesis 4 (2001) 289–298.